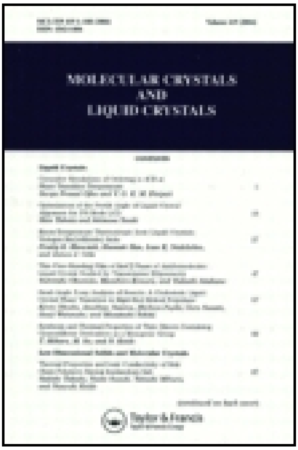

Molecular Crystals and Liquid Crystals Science and Technology. Section A. Molecular Crystals and Liquid Crystals

Publication details, including instructions for authors and subscription information:
http://www.tandfonline.com/loi/gmcl19

Investigation of Polarization-Induced Orientational Order and Surface Gratings in Liquid Crystalline AZO-Polymers

R. Macdonald [a] , R. Schulz [a] & C. Schreiber [a]

[a] Optisches Institut, Technische Universität Berlin, Strasse des 17. Juni 135, D-10623, Berlin, Germany

To cite this article: R. Macdonald, R. Schulz & C. Schreiber (2001): Investigation of Polarization-Induced Orientational Order and Surface Gratings in Liquid Crystalline AZO-Polymers, Molecular Crystals and Liquid Crystals Science and Technology. Section A. Molecular Crystals and Liquid Crystals, 359:1, 1-16

To link to this article: http://dx.doi.org/10.1080/10587250108035563

Mol. Cryst. and Liq. Cryst., 2001, Vol. 359, pp. 1-16
Reprints available directly from the publisher
Photocopying permitted by license only

Investigation of Polarization-Induced Orientational Order and Surface Gratings in Liquid Crystalline AZO-Polymers

R. MACDONALD, R. SCHULZ and C. SCHREIBER

Optisches Institut, Technische Universität Berlin, Strasse des 17.Juni 135, D-10623 Berlin, Germany

Polarization-induced orientational order in three different azopolymers is investigated and discussed with respect to the formation of surface relief gratings induced by holographic exposure. For this purpose the birefringence and dichroism induced by different light polarization, namely linear, elliptical or circular, has been studied. To determine the symmetry and the induced amount of orientational order the illuminated region is characterized by the scalar Maier-Saupe order parameter S. Tensor gratings were induced in these materials by holographic exposure with different kinds of polarization patterns and were investigated with polarization- and atomic force microscopy. The gratings are characterized by diffraction efficiencies as well as by depth and shape of the surface modulation. Large surface modulations (>2,5μm) and diffraction efficiencies (>90%) for a 5μm thick film were obtained.

Keywords: surface relief grating; photoorientation; order parameter; azobenzene; photopolymer

INTRODUCTION

Light-induced orientation of azo-dye containing polymers has been intensively studied during the last decade [1,2,3,4]. This photo-orientation process is explained to result from trans-cis-photoisomerization cycles of the azo-chromophores and orientational diffusion. The most obvious and prominent light polarization which has been reported for almost all investigations of this photo-alignment was linear, which lead to align the moieties with the long molecular axis perpendicular to the polarization direction. As a consequence, the illuminated polymer becomes birefringent as well as dichroic, which can be used to determine the induced orientation. Moreover, this photoorientation offers most fascinating opportunities in many fields of molecular optics and photonics like optical storage, holography, special light modulation or optical command surfaces for the alignment of liquid crystals.

Recently, it was reported [5,6,7,8] that the photo-reorientation process of the azo-moieties is accompanied by the formation of strong surface modulations during holographic grating experiments in side-chain liquid crystal polymers (SCLP). Several theoretical explanations have been proposed in which the formation of the gratings are explained by dipole-polarization interaction [9], pressure gradients due to inhomogeneous distribution of the free volume [10], directional displacements of the chromophores [11] and reorientation effects in combination with surface-tension [12]. But up to now no consistent theory was published, which is able to explain all observations connected with these phenomenon.

In the present paper, it is shown that different states of the polymerization, namely linear, elliptical or circular may lead to different uniaxial as well as biaxial orientational order. It is further studied, if the holographic exposure with different types of polarization gratings and the resulting spatial modulation in alignment (i.e. tensor gratings) are related to the formation of surface gratings.

EXAMINED POLYMERS AND FILM PREPARATION

The photo-orientational response of three different azo-containing side-chain-polymers (Fig. 1) to polarized light was examined. Polymer A is a homopolymer (100 mol% azo-dye) with an acrylate backbone which has a glass-transition temperature of 57°C and also phase transition temperatures at 83°, 108° and 159°C at which it turns isotropic. Polymer B consists of a methacrylate backbone and an azo-dye concentration of 70 mol%. The glass-transition temperature T_g is 60°C and it has a smectic phase up to 142°. Polymer C consist of a polycarbon-backbone with an azo-dye concentration of 5 mol%. The glass-transition temperature is above 170°C. It is an amorphous polymer and has no liquid crystalline phases.

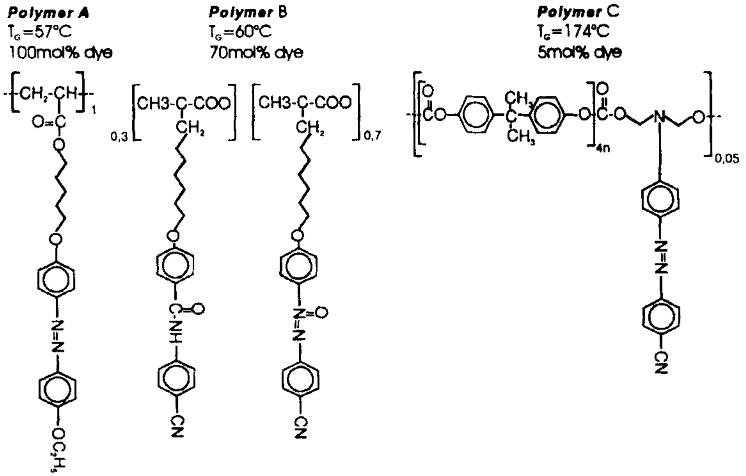

Fig. 1.: The chemical structure of the three investigated polymers.

For most of the following experiments thin isotropic films were prepared on glass substrates by spin-coating. A 10 wt% polymer-THF (Tetrahydrofuran) solution at 3000 RPM. Films prepared by this method had an thickness of approximately 1-2 μm and were macroscopically isotropic. The thickness was measured with a Dektak-instrument by scanning the depth of a small cut. With polymer A also thicker films have been prepared by splitting a glass-cell in which the polymer was filled before. This cell consists of two glass plates separated by spacers of 5µm thickness. The polymer was filled into these cells by heating it above the isotropic transition temperature and utilizing capillary forces. After the filling process the cells were cooled down rapidly by pressing them between two metal plates which were at liquid nitrogen temperature. By splitting the glass plates good quality films with 5µm thickness were obtained. It has to be mentioned that these films are not isotropic anymore. There was always a weak macroscopic orientation of the chromophores, probably caused by flow alignment during the filling process, leading to a weak birefringence which was observed with a polarization microscope before any further treatment or illumination of the film.

POLARIZATION INDUCED ORIENTATIONAL ORDER

As already mentioned above, the photoisomerization process is polarization selective. Assuming that the frequency of the linear polarized wave is more or less close to the π-π^* transition of the chromophores; only those azo-moieties undergo photoisomerization which have a transition moment component parallel to the optical field. Due to orientational diffusion during many trans-cis-trans cycles the angular site parallel to the optical field is emptied (angular hole burning). As a result, the trans chromophores are finally more or less aligned in a plane with the transition moments perpendicular to the optical field.

However the orientation of the chromophores within this plane is random. This kind of orientation is called oblate alignment, leading to a negative birefringence due to a smaller extraordinary refractive index with the investigated polymers (Fig. 2). The symmetry-axis is parallel to E. Described by the Maier-Saupe order parameter this orientation can be characterized by negative values with an optimum value of $S= -0.5$ in the case of perfect alignment.

If, on the other hand, circular polarized light is used, it is often claimed that no alignment is induced, or moreover, that alignment obtained with a linear polarized wave can be erased. However, for symmetry reasons, this is obviously not the case. Since the optical field, averaged over one oscillation period, covers the plane perpendicular to the wave propagation direction, the chromophores are now aligned perpendicular to that plane for the same arguments as given above. Consequently, all trans-moieties should finally point more or less along the propagation direction. This alignment is called prolate or homeotropic. The birefringence is positive with the polymers under investigation and the optical axis points along k. The maximum order parameter could be S=1 for perfect alignment.

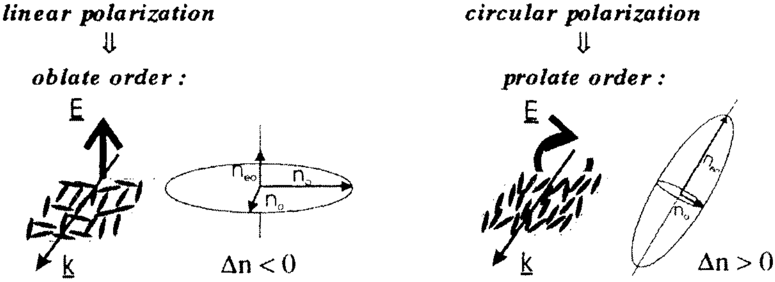

Fig. 2. Orientation of azo-chromophores by polarization selective trans-cis-photoisomerization.

It is worth to mention that the same uniaxial prolate alignment is expected for illumination with randomly polarized ("unpolarized") light for the same symmetry reasons as with circular polarized waves, whereas a biaxial alignment is obtained with elliptically polarized light.

In the following experiments the photo alignment was induced with an argon-ion laser emitting at a wavelength of 488nm. The laser spot was 2mm and the intensities were in the range of 0,5-1 W/cm^2. To ensure that heating effects in the polymer are not very important several experiments were made with less power (10-100 mW/cm^2). It turns out that the induced final alignment did not depend on intensity but was only a function of the absorbed energy. Therefore, thermal effects can be neglected.

$$S = \frac{\alpha_{\parallel} - \alpha_{\perp}}{\alpha_{\parallel} + 2\alpha_{\perp}} \qquad (1),$$

where α is the absorption coefficient and the indices $\parallel$, $\perp$ are with respect to the symmetrical axis of the induced orientation. This method was not applied in the case of prolate or homeootropic order, because of the quasi isotropic appearance for normal incident beams. Due to strongly angle-dependent surface-reflection we did not obtain accurate results with slanted samples. An alternative method to obtain information about the order is to determine the induced birefringence Δn of the sample by measuring the depolarization of a low-power HeNe-probe laser behind the polymeric sample at 633nm :

DETERMINATION OF POLARIZATION INDUCED ORDER

Two methods have be employed to determine the polarization induced order. The first one is connected with the angle-dependent absorption (dichroism) and the second one with the birefringence. By measuring the dichroism of the illuminated region we determined the oblate order [14] (Tab. 1):

$$\Delta n = \frac{\lambda_{HeNe}}{\pi d_{opt}} ArcSin\left[\sqrt{\frac{I_{\perp}}{I_{\perp} + I_{\parallel}}}\right], \qquad (2),$$

where d_{opt} is the optical thickness of the polymer and $\parallel$, $\perp$ are with respect to the polarization of the HeNe-laser.

For this purpose the polarization of the HeNe-laser was adjusted with an angle of 45° to the main axis (n_o and n_{eo}) of the refractive index-ellipsoid. The laser was expanded by a telescope and focused with a 100mm lens onto the sample to provide that the birefringence is measured over a region with homogeneous orientation. All polymers exhibited no significant absorption at 633nm and there was no indication that the HeNe laser had an influence on the alignment process. The change of the birefringence was monitored with a photodiode as a function of the exposure-time. The exposure was stopped when a maximum value was reached. The sample was set on a xyz-unit which could be rotated around the y-axis (Fig. 3). With this setup it was possible to measure the birefringence for different angles of incidence of the HeNe-laser.

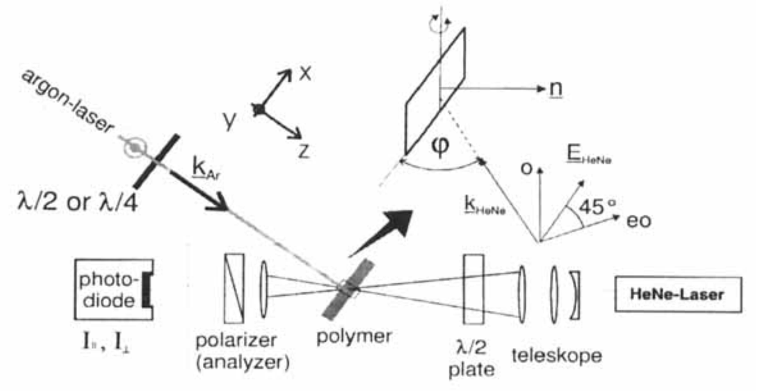

Fig. 3 : Experimental setup for birefringence measurements.

To determine the induced order from the birefringence it is necessary to know the difference between the main-axis refractive indices of the ellipsoid. For the determination of the oblate order it is necessary to know the difference between the refractive indices n_1 and n_2. $|n_1-n_2|$ can easily be determined by measuring the birefringence at normal incidence (z-axis). For the other two indices it would be necessary to measure the birefringence parallel to the polymer-surface (xy-plane). To overcome this problem we performed angle-dependent measurements and extrapolated the results to smaller angles. With our experimental setup the minimum angle was limited to $\alpha=35°$. With a parameterization of the index-ellipsoid it is possible to derive a fit-formula and extrapolate this measurement to smaller angles. The extraordinary refractive index as a function of the HeNe-angle of incidence is given by the following formula.

$$n_{ao}(\varphi) = n_1 / \sqrt{\mathrm{Sin}^2[\varphi] + \frac{n_1^2 \cdot \mathrm{Cos}^2[\varphi]}{n_3^2}} \tag{3}$$

To obtain detailed information about the polarization induced orientation of the azo-molecules we changed the polarization of the argon-laser from linear to circular and measured the birefringence afterwards as a function of the angle of incidence of the probe-laser. The polarization is changed in four steps from linear to circular by adjusting a quarterwave-plate and it is described by the elliptically-parameter ε which is $\varepsilon=0°$ for linear polarized light and $\varepsilon=45°$ for circular polarized light. It is also possible to determine the symmetry of the induced order if the experiments are made with two different orientations of the film. If the film is rotated 90° around the surface normal n the main-axis of the index-ellipsoid (ordinary and extraordinary) are changing their role. The first film-orientation is called side-view and the second one top view (Fig. 4).

To calculate the order parameter from these experiments we combined the results of the birefringence with the results from the dichroism-measurements. If the birefringence is small against the refractive index of the polymer (which is fulfilled in our case since $\Delta n \approx 0{,}1 < n_{iso} = 1{,}6$) it is possible to derive a relation between the order parameter S and the birefringence Δn :

$$S = \frac{\varepsilon_{\parallel} - \varepsilon_{\perp}}{\varepsilon_l - \varepsilon_q} \quad \text{and}$$

$$\varepsilon_{\parallel} - \varepsilon_{\perp} = (n_{\parallel} - n_{\perp})(n_{\parallel} + n_{\perp}) = \Delta n \;\; (2n_{\perp} + \Delta n) \approx 2n_{\perp}\Delta n \tag{4}$$

$$\Rightarrow S \approx \frac{n_{\parallel} - n_{\perp}}{\varepsilon_l - \varepsilon_q} \, 2n_{\perp} = k \cdot \Delta n$$

Since S and Δn are known for the oblate order from the dichroism experiments the constant k and the order parameter S for the prolate order can be determined.

In Fig. 4 the results of the angle-dependent measurement of the birefringence are shown exemplary for polymer A. Results for all investigated polymers are summarized in Tab. 1.

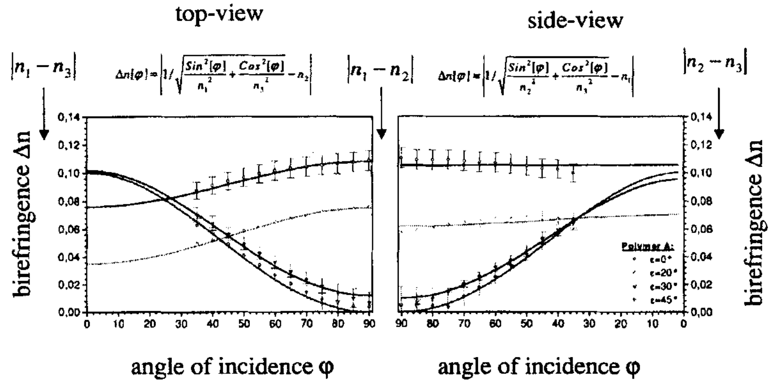

$$\underline{\underline{a}}^{PolymerA}_{prolate} = 0{,}39\cdot\begin{pmatrix} -\frac{1}{3} & 0 & 0 \\ 0 & -\frac{1}{3} & 0 \\ 0 & 0 & \frac{2}{3} \end{pmatrix} \qquad \underline{\underline{a}}^{PolymerA}_{oblate} = -0{,}41\cdot\begin{pmatrix} \frac{2}{3} & 0 & 0 \\ 0 & -\frac{1}{3} & 0 \\ 0 & 0 & -\frac{1}{3} \end{pmatrix}$$

Fig. 4 : Angle dependent measurement of the birefringence of polymer A for four different polarization states ($\varepsilon = 0°$-$45°$) of the pump-light (488nm, 1W/cm^2) and resulting orientation-tensor $\underline{a} = S\cdot\left(\overrightarrow{L}\overrightarrow{L}\right)$. The results were fitted with formula (3).

With linear polarization ($\varepsilon=0$) all polymers exhibit a good oblate alignment with approximately $\Delta n=|n_2-n_1|=0{,}1$. For the side-view, i.e. rotation around the polarization axis, the birefringence remains constant within our experimental accuracy. This is the expected symmetry for an oblate orientation. It is worth to note that the order parameter of polymer A is twice as high (S=-0,41) as for polymer B (S=-0,22) and C (S=-0,21), i.e. the induced order was 50-80% of the ideal oblate orientation. With circular polarized light (ε=45°), the induced alignment in polymer A shows a strong angle-dependence which is indicated by a rise from $|n_1-n_2|=0$ to $|n_1-n_3|=|n_2-n_3|=0{,}1$. This is corresponding to an order parameter of S=0,39 which is 39% of the optimum theoretical value.

As a result it seems to be more difficult to induce a prolate than an oblate alignment, depending however on the different polymer. In particular for Polymer B and C the prolate order parameter is only in the range of 4%-5% of the optimum value of 1, i.e. the order is rather weak and not very different from an isotropic distribution. For elliptical polarization (e.g. ε=20°) the induced alignment is some combination of oblate and prolate order and the induced order is biaxial, which is also displayed in the results.

Tab. 1 : Birefringence and calculated order parameter S for oblate and prolate order at photostationary equilibrium for all three polymers.

	oblate order $n_\parallel - n_\perp$	oblate order S	prolate order $n_\parallel - n_\perp$	prolate order S
Polymer A	**-0,105** ± 0,008	**-0,41** ± 0,01	**0,10** ± 0,008	**0,39** ± 0,08
Polymer B	**-0,120** ± 0,008	**-0,22** ± 0,01	**0,020** ± 0,008	**0,04** ± 0,02
Polymer C	**-0,080** ± 0,007	**-0,21** ± 0,01	**0,020** ± 0,008	**0,05** ± 0,02

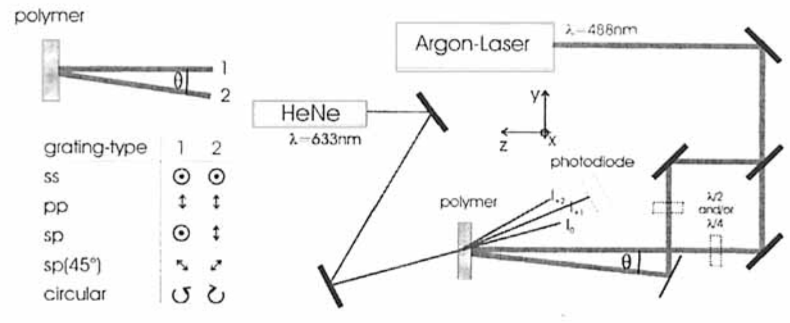

Fig. 5 : Experimental setup for the holographic experiments and definition of the grating types.

SURFACE RELIEF GRATINGS

A holographic setup was used for the grating-experiments. Intensity gratings as well as polarization gratings [15] were applied. For the realization of polarization gratings halfwave- and/or quarterwaveplates were inserted into the beams (see Fig. 5). Dielectric mirrors have been used to minimize depolarization effects. The beam-intersection angle was approx. 1°, which leads to a grating period of 25µm.

The excitation region had a diameter of 2mm and the intensities were in the range of 0,1-1W/cm^2. The diffraction efficiency in the transmission mode was probed with a polarized low power HeNe-laser at 633nm. Due to the fact that the diffraction efficiency is strongly dependent on the polarization of the probe laser [16], we adjusted the HeNe polarization for each grating condition so that a maximum diffraction was reached. For thin films the intensity of the first diffraction-order was monitored as a function of exposure time with a photodiode. Once the diffraction signal reached a maximum, the excitation was stopped. Because of the large diffraction efficiencies for thicker films (d=5µm) the decrease of the intensity in the zero diffraction-order was monitored in these cases. Results for the thin film diffraction efficiencies are summarized in Tab. 2. For all three polymers the grating obtained with circularly polarized beams of opposite handiness provides the largest diffraction efficiencies whereas the pure intensity grating yields the smallest values. Between ss- and pp intensity gratings there were no differences in the diffraction efficiencies, which can be explained by the small intersection angle of approx. 1°. Comparing the three polymers, material A gives the best results.

Tab. 2 : Thin-film 1st order diffraction efficiencies for three different recording conditions

	ss	sp	circular
Polymer A	0,2%	5,5%	12%
Polymer B	0,2%	1,5%	3,5%
Polymer C	1%	3.3%	7%

The observed dependence of diffraction efficiency on the type of excitation grating was also reported by other groups [7,8,12,13] and can be explained by the variation of the polarization in case of the polarization gratings and the resulting alignment of the azo-chromophores as discussed above. Decisive for the resulting diffraction efficiency is the change of the refractive index in the direction perpendicular to the grating grooves (x).

Clearly, the diffracted intensities in our experiment can not be explained only by bulk birefringence modulations, e.g. Δn of 0,1 would lead to an diffraction efficiency of only 6% for a 1µm layer. Also the larger efficiencies obtained with polymer C compared with polymer B are in contrast to the determined photoinduced birefringence (Tab. 1), where Polymer B had higher values than polymer C. So we checked the polymers for surface relief gratings with atomic force microscopy.

For polymer C we observed with all three types of gratings periodic surface modulations reaching from 10nm depth for ss-polarization to 100nm with circularly polarized beams. The surface clearly exhibits a sinusoidal modulation in these cases. For ss and circular recording polarization the grating spacing was consistent with the expected spacing of the interference pattern. For the sp-grating we observed double the period of the expected fringe pattern [12].

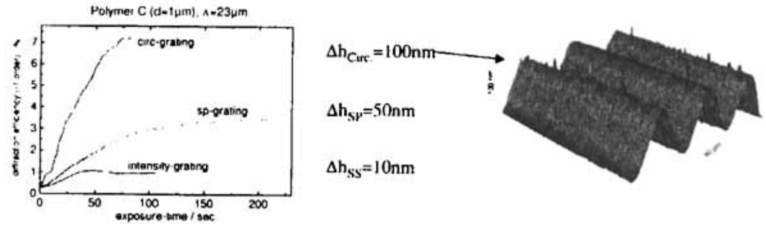

Fig. 6 : **1st order diffraction efficiencies as a function of exposure time, depth modulations and AFM-scan of the surface relief for the circular recording conditions for polymer C.**

Surprisingly no smooth surface gratings could be obtained with polymer A. It turns out that this may be due to the fact that the surface quality of the film was poor. The surface gratings were very uneven with spot-like structures of approx. 1µm in size. These effect can be explained with the appearance of microdomains during the exposure due to the liquid crystalline character of the polymer and was confirmed by the fact, that the illuminated regions show some strong scattering and were not transparent anymore [17]. Anyhow a periodic depth-modulations for polymer A were also in the range of 100nm. The film of polymer B was covered with many microscopic holes (with a diameter of approx. 0,5µm) which might have the origin in a reaction during the drying process, where the solvent evaporates out of the polymer. This phenomenon was observed only with polymer B.

For the thick films, which were only prepared with polymer A so far, we obtain results which in some aspects are different to the thin-film results. We used the same experimental setup as for the thin films. With these films we succeed to induce significant surface reliefs even with pure intensity gratings (Fig. 7) up to huge 2,5µm depth modulation. The results for all recording conditions with the 5µm films are summarized in Tab. 3. In all cases the depletion of the zero-order beam due to diffraction into higher orders was more than 90%. The characteristic dependence for the diffraction efficiency upon the recording polarization conditions was not observed with the thick films. In fact the largest modulations were induced with the ss- and the sp(45°)-conditions. This behavior may be explained by the pre-orientation of the films due to the filling process, as mentioned above. As a result these films already have a macroscopic non-uniform orientation and birefringence which yields a refractive-index gradient even before the exposure. These conditions seems to be important for the building of the surface reliefs. Also the thick films do not exhibit the disturbed surface like the spin-coated films

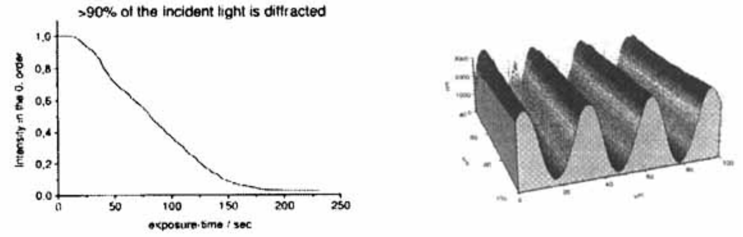

Fig. 7 : **Zero-order intensity as a function of exposure time, depth modulations and AFM-scan of the surface relief for the ss-recording conditions for a 5µm thick film of polymer A.**

of polymer A. In these cases the pre-alignment of the illuminated area seems to be of more importance than the type of the applied polarization grating.

Tab. 3 : Summary of the measured grating characteristics for photo-induced gratings in polymer A with d=5μm

configuration	depth-modulation	period	form
ss	2,5μm	25μm	harmonic
pp	0,6μm	25μm	harmonic
sp	0,6μm and 0,3μm	12,5μm	harmonic
sp(45°)	2,7μm	25μm	anharmonic
circular	0,9μm	25μm	harmonic

It is obvious that with polymer A the highest photoinduced order and the largest surface modulations have been obtained. A possible explanation for this behavior is the low molar mass of polymer A (12 kg/mol). For short polymer chains a migration over some distance seems more probable than for long chains [10].

Due to the relatively large grating period of 25μm it was also possible to examine the birefringence gratings with a polarization microscope. A characteristic dependency of the birefringence grating profile as a function of the sample orientation with respect to the polarizers has been observed. For example, in the case of a circular orthogonally grating excitation the birefringent regions are "moving" across the sample, if the sample is rotated around the surface normal. This is a consequence of the rotating linear polarization state along the grating pitch during holographic exposure, which leads to aa oblate alignment order with a rotating optical axis. To give another example, for linear orthogonally gratings the regions illuminated with circular polarized light are always dark, due to their homeotropic alignment, whereas the regions illuminated with linear polarized light are changing from bright to dark. By carefully studying these polarization microscopic pictures, all types of oblate as well as prolate alignment which have been discussed above have been also identified in the fringes of the induced holographic polarization gratings.

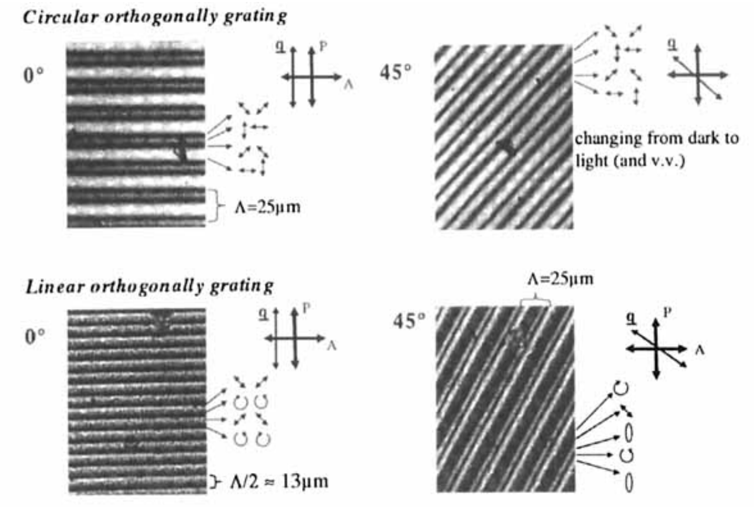

Fig. 8 : **Pictures of the birefringence grating-profile for a circular orthogonally grating and linear orthogonally grating under a polarization microscope for two kinds of sample orientations and identification of the different polarization regions. P : polarizer; A: analyzer; q: grating vector.**

CONCLUSION

Polarization induced orientational order in three different azo-polymers has been investigated. The symmetry and the amount of alignment has been determined from birefringence and dichroism measurements. The later was characterized by the Maier-Saupe order parameter S. With linear polarized light all polymers exhibit a good oblate alignment (S=-0,4 to -0,2). For circular polarized light a good prolate orientation was induced only in polymer A (S=0,39). For the other two polymers only a weak prolate order was observed (S=0,04-0,05).

A spatially periodic variation of the polarization state or the intensity has been realized by holographic exposure with different kind of polarization gratings to study the formation of surface relief modulation. A characteristic dependence of the diffraction efficiencies upon the recording polarization conditions was observed. It turns out, that a grating modulation of the optical axis seems to be important for the formation of strong surface gratings. With 5μm-thick films of polymer A we obtained a record high modulation depth of 2,7μm, which is more than 50% of the initial film thickness.

Acknowledgements

We sincerely thank Dr. J. Rübner, Technische Universität Berlin, Institut für Technische Chemie, for the synthesis of Polymer A and B; and Dr. R. Ruhmann, formally Institut für Angewandte Chemie Adlershof Berlin, for the synthesis of Polymer C.

References

[1] L. Nikolova, T. Todorov N. Tomova; *Appl. Opt.* Vol. **23**, 4588 (1984).

[2] M. Eich, J.H. Wendorf, B. Reck, H. Ringsdorf; *Macromol. Chem.*, Rapid Commun. **8**, 59 (1987).

[3] M. Eich, J.H. Wendorf:, *J. Opt. Soc Am. B,* **7**, 1428 (1990).

[4] P. Rochon, J. Gosselin, A. Natansohn, and S. Xie, *Appl. Phys. Lett.* **60,** 4 (1992).

[5] P. Rochon, E. Batalla, A. Natansohn, *Appl. Phys. Lett.* **66** (2), 1995.

[6] D.Y. Kim, S.K. Tripathy, Lian Li, J. Kumar, *Appl. Phys. Lett.* **66** (10), 1166, 1995.

[7] X.L. Jiang, D.Y. Kim, S.K. Tripathy, Lian Li, J. Kumar, V. Shivshankar, *Appl. Phys. Lett.*, **68**, 2618, (1996).

[8] C. Barrett, P. Rochon, A. Natansohn, *J. Phys. Chem.* **100**, 8836 (1996)..

[9] J. Kumar, L. Li, X.L. Jiang, D.Y. Kim, S.K. Tripathy, T.S. Lee, *Appl. Phys. Lett.*, **72**, 2096 (1998).

[10] C. Barrett, P. Rochon, A. Natansohn, *Polymer Preprints* **38,** 542 (1998).

[11] P. Lefin, C. Fiorini, *Opt. Mat.*, **9**, 323 (1998).

[12] T.G. Pedersen, P.M. Johansen, N.C.R. Holme, S. Hvilsted, P.S. Ramanujam, *Phys. Rev. Lett.*, **80** Number 1, 89–93 (1998).

[13] D.Y. Kim, T.S. Lee, *SPIE* Vol. 2998, 195 (1997).

[14] L.M. Blinov, V.A. Kizel et.al, *Sov. Phys. Crystallogr.*, **20,** No. 6, 750 (1974)..

[15] H.J. Eichler, P. Günter, D.W. Pohl, Springer, Berlin (1986).

[16] I. Naydenova, L. Nikolova, T. Todorov, N.C.R. Holme, P.S. Ramanujam, *J. Opt. Soc. Am. B*, **15**, 1257 (1999).

[17] J. Stumpe, private communication.